Astronomy & Astrophysics manuscript no. VII_Nilsson_rev
January 8, 2019

Experimental transition probabilities for 4p - 4d spectral lines in V II

H. Nilsson[1], J. Andersson[2], L. Engström[3], H. Lundberg[3], and H. Hartman[1,4]

[1] Lund Observatory, Lund University, Box 43, 22100 Lund, Sweden
e-mail: hampus.nilsson@astro.lu.se

[2] Department of Physics, University of Gothenburg, SE-412 96 Gothenburg, Sweden

[3] Department of Physics, Lund University, Box 118, 22100 Lund, Sweden

[4] Applied Mathematics and Material Science, Malmö University, 20506 Malmö, Sweden

Received December 07, 2018; accepted ?

ABSTRACT

Aims. We aim to measure lifetimes of levels belonging to the $3d^3(^4F)4d$ subconfiguration in V II, and derive absolute transition probabilities by combining the lifetimes with experimental branching fractions.
Methods. The lifetimes were measured using time-resolved laser-induced fluorescence in a two-photon excitation scheme. The branching fractions were measured in intensity calibrated spectra from a hollow cathode discharge lamp, recorded with a Fourier transform spectrometer.
Results. We report lifetimes for 13 levels at an energy around 73000 cm^{-1}. Absolute transition probabilities of 78 lines are derived by combining the lifetimes and branching fractions. The experimental values are compared with theoretical data from the literature.

Key words. atomic data – line: identification – methods: laboratory: atomic – techniques: spectroscopic

1. Introduction

Vanadium has a high abundance in many astrophysical objects. The solar abundance of vanadium is A_V=3.99 (A_V=log[N_V/N_H] + 12) (Lodders 2009), and spectral lines of vanadium are seen in the spectra of for example χ-Lupi (Brandt et. al. 1999) and η Carinae (Hartman et al. 2004). The 4p-4d lines from the highly excited levels reported in this paper are important to benchmark theoretical calculations of spectroscopic data and to test stellar atmosphere models.

The present paper is part of an ongoing project where lifetimes of high excitation levels in the iron-group elements are measured (Engström et al. 2014; Hartman et al. 2015; Lundberg et al. 2016; Quinet et al. 2016; Hartman et al. 2017).

The ground configuration in V II is $3d^4$, closely followed by $3d^34s$, starting at 2605 cm^{-1}. The first odd configuration is $3d^34p$ at 34592 cm^{-1}. The even $3d^35s$ and $3d^34d$ configurations start at 69146 cm^{-1} and 72448 cm^{-1}, respectively. An extensive analysis of the V II term system was reported by Thorne et al. (2013) based on high resolution Fourier transform spectroscopy. They reported energies for 176 even and 233 odd levels, and wavelengths for 1242 classified spectral lines.

Previous work on lifetimes and transition probabilities in V II include Roberts et al. (1973) who reported absolute and relative oscillator strengths derived by combining lifetimes measured with the beam foil technique and branching rations measured in a stabilized arc. In two papers Goly & Weniger (1981, 1984) published absolute log(gf)-values for 99 lines measured in a wall-stabilized arc. The same technique was utilized by Wujec & Musielok (1986), who reported transition probabilities for 211 lines in V II. Karamatskos et al. (1986) reported lifetimes of 12 levels measured by laser excited fluorescence from a sputtered metal vapor. Schade et al. (1987) reported 13 lifetimes measured with selective laser excitation and time resolved observation of the fluorescence signal. Biemont et al. (1989), measured six lifetimes with time resolved laser induced fluorescence (TR-LIF) and branching fractions (*BF*s) from emission spectra recorded with the Kitt Peak National Observatory 1-meter Fourier transform spectrometer. Combining the lifetimes with the *BF*s they obtained a total of 133 V II transition probabilities. Xu et al. (2006) reported TR-LIF lifetimes for 11 levels in V II. Den Hartog et. al. (2014) reported lifetimes of 31 levels in V II (and for 168 lifetimes of levels in V I) measured using TR-LIF. Wood et. al. (2014) reported log(gf)-values from 203 lines, derived by combining lifetimes from the literature and branching fractions measured in spectra recorded with the Fourier transform spectrometer at the Kitt Peak National Solar Observatory and an echelle spectrometer at the University of Wisconsin. All these papers report on lines originating from the first excited odd configurations, $3d^34p$ or $3d^24s4p$ except for 12 lines reported by Wujec & Musielok (1986) between the, 4p - 4d and 4p - 5s configurations. A critical compilation of V II can be found in Saloman & Kramida (2017). In this work we report the first measurements of lifetimes and *BF*s for higher even levels in V II.

2. Laboratory measurements

2.1. Lifetimes

The lifetimes were measured at the High Power Laser Facility at Lund University. The experimental set up for two-photon excita-

Article published by EDP Sciences, to be cited as https://doi.org/10.1051/0004-6361/201834795

tions has been described in detail in for example Engström et al. (2014) and only a brief overview will therefore be given here.

The V^+ ions were produced in an ablation plasma created by focusing a frequency doubled ND:YAG laser (Continuum Surelite) on a rotating target made out of vanadium. The target was placed in a vacuum chamber with a pressure of 10^{-4} mbar. The levels were populated in a two-photon excitation scheme, using a frequency doubled injection seeded ND:YAG (Continuum NY-82) pumping a Continuum ND-60 dye laser using a DCM dye. The output was temporally compressed using stimulated Brillouin scattering in water resulting in a FWHM of 1.2 ns. All lasers operate at 10 Hz and the relative timing was controlled with a delay generator. The excitation laser was adjusted both in time and space to overlap with the ablation plasma, approximately 5 mm above the vanadium sample in the target chamber.

The fluorescence signal was filtered out with a 1/8 m monochromator and detected perpendicular to the excitation and ablation lasers with a fast multichannel plate photo multiplier tube (Hamamatsu R3809U). The signal was recorded with an oscilloscope (Tektronix DPO 7254). In addition, the shape of the excitation pulse was simultaneously recorded with a fast diode. The decay curves were analyzed using the code DECFIT (Palmeri et al. 2008) where we fit a single exponential decay convoluted by the measured excitation laser pulse and a constant background. Each measurement was obtained by accumulating 1000 laser shots, and the final lifetimes were derived by averaging 10-20 measurements performed over several days.

To verify that the correct level was excited we checked that all expected decay channels could be observed and, where possible, the lifetime was measured in all sufficiently intense decay channels. Furthermore, in some cases it was possible to utilize several excitation schemes to reach the level.

In the measurements of the e^5P levels the fluorescence signal and the excitation pulse were close in wavelength and scattered laser light was therefore present in the recorded signal. This was corrected for by turning off the ablation laser and record the scattered laser light, which could be subtracted from the measured lifetime curve.

The lifetimes obtained are given in Table 1. The different excitation schemes and detection channels are included in columns 3 and 4. The quoted uncertainties are based on the variation between the repeated measurements. Our experimental lifetimes are compared with the semi empirical values calculated by Kurucz (1995, 2013).

2.2. Branching fractions and transition probabilities

The BF is defined as:

$$BF_{ul} = A_{ul} / \sum_{k=1} A_{uk}, \quad (1)$$

where u and l denotes the upper and lower level, respectively and A the transition probability. However, if the spectra are intensity calibrated, (1) can be rewritten as:

$$BF_{ul} = I_{ul} / \sum_{k=1} I_{uk} \quad (2)$$

where I_{uk} is the calibrated intensity. Finally, since

$$\sum_{k=1} A_{uk} = 1/\tau_u, \quad (3)$$

the desired transition probability can be obtained from:

$$A_{ul} = BF_{ul}/\tau_u. \quad (4)$$

The transition probability can thus be derived if the lifetime of the upper level is known, and if all lines from this level can be measured. The last requirement is rarely possible since all lines will contribute to the sum, but not all lines are strong enough to be measured in the laboratory. The contribution from lines not measured is called the "residual", which can be estimated using theoretical calculations.

The BFs were measured from spectra recorded with a Fourier transform spectrometer (Chelsea Instruments FT 500). The maximum path difference between the mirrors is 20 cm, giving a resolving power of 10^6 at 2000 Å. Free V^+ ions were produced in a hollow cathode discharge (HCD) lamp. Spectra were recorded using neon, argon and a mixture of both neon and argon as carrier gases at different gas pressures (0.5–2.0 Torr) and currents (0.1–1.0 A). No self absorption could be seen using these values. The low excitation 4s-4p lines gave nearly the same intensities with neon and argon, while the high excitation 4p-4d lines were clearly much stronger running the HCD with argon at low currents and a pressure of 2 Torr. This enhancement could be caused by selective excitation due to charge transfer (Johansson & Litzén 1980). The spectra were intensity calibrated with a deuterium lamp with a known spectral intensity distribution measured at the Physikalisch-Technische Bundesanstalt, Berlin, Germany with an uncertainty of 4%. All lines from the measured 4d levels fall in an interval between 35000 and 38600 cm^{-1} (2595–2850 Å). However, they show up as two distinct groups, one around 36000 cm^{-1} where the upper 4d levels combine with 4p z^3D, z^5F and z^5D, and one group around 38000 cm^{-1}, with combinations to z^5G. This is illustrated in Fig. 1. The intensity of the spectral lines was measured as the area of a fitted line profile obtained using the code GFit (Engström 1998). The residuals (ranging from 0.003 to 0.11) were estimated using the theoretical results of Kurucz (1995) and are included in Table 2. Even though the uncertainty in these values may be quite large their influence on the BFs is small in most cases.

Vanadium has two naturally occurring isotopes, ^{51}V (99.75%) and ^{50}V (0.25%). The dominant isotope, ^{51}V, has a nuclear spin $I = 7/2$ which, combined with the large nuclear magnetic moment ($\mu/\mu_N = 5.1514$), give rise to a noticeable hyperfine structure pattern in many lines. However, the lines in this study did not show any resolved hyperfine structure. This is due to the weak interaction with the nucleus for the 4d and 4p electrons, resulting in a smaller hyperfine splitting than the Doppler width of the lines.

One minor experimental problem concerns the strong z^5F_4 – e^5G_5 (λ 2771.359) transition which is blended by the line z^5F_1 – e^5F_2 (λ 2771.373) resulting in a slightly too large measured BF. However, the extra intensity added should only give rise to a small contribution. Assuming that the z^5F_1 – e^5F_2 transition has a branching fraction of 0.06 (Kurucz 1995) the change in the BF for the z^5F_4 – e^5G_5 line will be from 0.405 to 0.390. In the newer calculation (Kurucz 2013) the BF of the z^5F_1 – e^5F_2 line is even less, only 0.016. We have therefore not corrected for this, although we have increased the uncertainty accordingly.

The total uncertainty in the transition probabilities span between 6 and 26 %, and are estimated as suggested by Sikström et al. (2002), including the uncertainty in the lifetimes, area measurement and intensity calibration. The observed branching fractions and derived $\log(gf)$-values are presented in Table 2 and compared with the theoretical results of Kurucz (1995, 2013).

3. Discussion

The only available complete theoretical investigations involving the 4d levels in V II are the two calculations by Kurucz (1995) and Kurucz (2013), henceforth referred to as K95 and K13. Both are performed with a modified version of the code by Cowan (1981) and use experimental level energies to optimize the values of some radial integrals. All our 78 *BF*s are compared with K95 in Fig. 2 and with K13 in Fig. 3. The standard deviations (σ) are 0.048 and 0.054 for K95 and K13, respectively. Although the two calculations have almost the same overall standard deviation, a more detailed comparison reveals interesting differences.

It can be seen in Table 2, that for lines from e^5P, the values from K13 are in significantly better agreement with our results (σ = 0.019) than K95 (σ = 0.088). This is especially clear when looking at the lines from the e^5P_3 level. For the z^3D_3-e^5P_3 intercombination line, the experimental *BF* is 0.098 while the theoretical values are 0.230 and 0.092 for K95 and K13, respectively. For the z^5D_4-e^5P_3 the experimental *BF* is 0.719 compared to the K95 value of 0.492 and the K13 of 0.692. Furthermore, the differences can be seen in Table 1, where the lifetimes from K13 are in better agreement with our experimental values for the e^5P term than K95, particularly for the e^5P_3 level which deviates from the other e^5P levels. The most likely explanation for the latter discrepancy is that the published transition probability for the strong z^5D_4-e^5P_3 line is not that calculated in K95 but the experimental value from Martin et al. (1988) which is, in turn, rescaled form Wujec & Musielok (1986). This experimental transition probability is clearly too low. The same substitution of experimental data has been done for the z^5D_3-e^5P_2 transition. These two points are marked with blue circles in Fig. 2. If we assume that the lifetime of the three e^5P levels are the same and recalculate the theoretical *BF*s we find that the standard deviation for K95 is reduced to 0.023, that is, almost identical to K13 (σ=0.019).

For the lines depopulating e^5F and e^5G the K95 calculations gives in general a better agreement with our experimental values, except for z^3D_3-e^5G_4 where again the K13 value is taken from Martin et al. (1988). This point is marked with a red circle in Fig. 2 and 5. The standard deviation for K95 is σ = 0.036 while it is σ = 0.059 for K13. The larger scatter when comparing the experimental *BF*s with K13 is clearly seen in Figs. 4 and 5. Thus, a somewhat surprising conclusion is that the older calculation in K95 is actually to be preferred over the newer K13, at least when it comes to the 4p - 4d transitions. For the lifetimes in e^5F and e^5G Table 1 shows that K95 overestimates the values by about the same amount that K13 underestimates them, although both are very close to the experimental results within the estimated uncertainties. But it is important to understand that the complexity of the iron group elements makes it very hard to calculate accurate transition probabilities and it is therefore necessary to benchmark the calculations with experimental measurements.

4. Summary

In this paper we report the first laboratory measurements of lifetimes for levels belonging to the $3d^34d$ configuration in V II. A total of 13 lifetimes are measured and given in Table 1. The combination of the lifetimes and *BF*s measured in spectra recorded from a hollow cathode discharge lamp have yielded transition probabilities of 78 4p-4d spectral lines presented in Table 2. A comparison with available theoretical calculations Kurucz (1995) and Kurucz (2013) illustrates the difficulties in the complex term systems of the iron group elements and the need for experimental data to benchmark the results.

Acknowledgements. This work was supported by the Swedish Research Council through the Linnaeus grant to the Lund Laser Centre and the Knut and Alice Wallenberg Foundation. HH gratefully acknowledges the grant no 2016-04185 from the Swedish Research Council.

References

Biémont, E., Grevesse, N., Faires, L. M., Marsden, G., Lawler, J. E., & Whaling, W., 1989, Astron. Astrophys., 209, 391
Cowan, R. D., 1981, The Theory of Atomic Structure and Spectra (Berkeley Univ. of California Press)
Brandt, J.C., Heap, S.R., Beaver, E.A., Boggess, A., Carpenter, K.G., Ebbets, D.C., Hutchings, J.B., Jura, M., Leckrone, D.S., Linsky, J.L., Maran, S.P., Savage, B.D., Smith, A.M., Trafton, L.M., Walter, F.M., Weymann, R.J., Proffitt, C.R., Wahlgren, G.M., Johansson, S.G., Nilsson, H., Brage, T., Snow M. and Ake, T.B., 1999, The Astronomical Journal, 117, 3, 1505
Den Hartog, E.A., Lawler, J.E. and Wood, M.P., 2014, The Astrophysical Journal Supplement Series, 215:7
Engström, L., 1998, Lund Reports in Atomic Physics (LRAP-232) Atomic Physics, Lund University. http://kurslab-atom.fysik.lth.se/Lars/GFit/Html/index.html
Engström, L., Lundberg, H., Nilsson, H., Hartman, H. and Bäckström, E., 2014, Astron. Astrophys., 570, A34
Goly, A., Weniger, S., 1981 J. Quant. Radiat. Transfer, Vol 25, 381
Goly, A., Weniger, S., 1984 J. Quant. Radiat. Transfer, Vol 32, No 1, 61
Hartman, H., Gull, T., Johansson, S., Smith, N. and the Eta Carinae Treasury Project Team, 2004, Astron. Astrophys., 419, 215
Hartman, H., Nilsson, H., Engström, L. and Lundberg, H., 2015, Astron. Astrophys., 584, A24
Hartman, H., Engström, L. and Lundberg, H., Nilsson, H., Palmeri, P., Quinet, P., Fivet, V., Malcheva, G., and Blagoev, K., 2017, Astron. Astrophys. 2017, 600, A108
Johansson, S. & Litzén, U., 1980, J. Phys. B: Molec. Phys. 13, L253
Karamatskos, N. , Michalak, R. , Zimmermann, P., Kroll, S. & Kock, M., 1986, Z. Phys. D, 3, 391
Kurucz, R. L., 1995, Atomic spectral line data from CD-ROM No. 23. Available at http://www.cfa.harvard.edu/amp/ampdata/kurucz23/sekur.html
Kurucz, R. L., 2013, http://kurucz.harvard.edu/atoms/2301/
Lodders, K., Palme, H., and Gail, H.-P., 2009, Landolt-Börnstein, New Series, Vol. VI/4B, Chap. 4.4, Abundances of the Elements in the Solar System, ed. J. e: Trümper (Springaer-Verlag, Berlin), 560-630
Lundberg, H., Hartman, H., Engström, L., Nilsson, H., Persson, A., Palmeri, P., Quinet, P., Fivet, Malcheva G. and Blagoev, K., 2016, MNRAS 460, 1, 356
Martin, G.A., Fuhr, J.R., and Wiese, W.L., 1988, Journal of Physical and Chemical Reference Data, Vol 17
Palmeri, P., Quinet, P., Fivet, V., Biémont, É., Nilsson, H., Engström, L., and Lundberg, H., 2008, Phys. Scr., 78, 015304
Quinet, P., Fivet, V., Palmeri, P., Engström, L., Hartman, H., Lundberg, H., and Nilsson, H., 2008, Phys. Scr., 78, 015304
Roberts, J. R., Andersen, T. & Sorensen, G., 1973, Astrophys. J., 181, 587
Saloman, E.B., and Kramida, A., 2017, The Astrophysical Journal Supplement Series, 231:19
Schade, W., Langhans, G. & Helbig, V., 1987, Phys. Scr., 36, 890
Sikström, C. M., Nilsson, H., Litzén, U., Blom, A. & Lundberg, H., 2002, J. Quant. Spectrosc. Radiat. Transfer, 74, 355
Thorne, A.P., Pickering, J.C. & Semeniuk, J.I., 2013, The Astrophysical Journal Supplement Series, 207:13
Wood, M.P, Lawler, J.E., Den Hartog, E.A., Sneden, C., & Cowan, J.J., 2014, The Astrophysical Journal Supplement Series, 214:18
Wujec, T. & Musielok, J., 1986a, J. Quant. Spectrosc. Radiat. Transfer, 36, 7
Xu, H.-L., Jiang, Z.-K. & Lundberg, H., 2006, J. Opt. Soc. Am. B, 23, 2597

Table 1. Experimental details and the measured lifetimes of the $3d^3(^4F)4d$ levels in V II.

Level	E^a [cm^{-1}]	Excitation λ^b_{air} [nm]	Detection λ^c_{air} [nm]	τ_{exp} [ns]	τ^d_{th} [ns]	τ^e_{th} [ns]
e^5P_1	72518	285.98, 286.32	283[f]	1.95 ± 0.15	2.17	1.91
e^5P_2	72674	285.35, 285.68	283[f]	1.95 ± 0.15	2.39	1.89
e^5P_3	72909	284.73, 285.22	280, 283[f]	1.87 ± 0.15	4.13	1.88
e^5F_1	72839	284.68	275	1.90 ± 0.15	2.04	1.79
e^5F_2	73027	284.74	261, 275	1.93 ± 0.15	2.00	1.76
e^5F_3	73146	284.91	276	1.94 ± 0.15	2.00	1.77
e^5F_4	73279	284.37, 285.16	262, 277	1.92 ± 0.10	2.01	1.77
e^5F_5	73417	284.60	276	1.87 ± 0.10	2.03	1.78
e^5G_2	72878	284.52	261, 278	1.87 ± 0.20	2.04	1.78
e^5G_3	72951	284.56	276, 278	1.98 ± 0.15	2.04	1.79
e^5G_4	73064	285.24	277, 279	1.80 ± 0.15	2.34	1.79
e^5G_5	73223	285.38	277, 280	1.99 ± 0.15	2.05	1.79
e^5G_6	73500	284.27	263	1.98 ± 0.10	2.03	1.77

[a]Thorne et al. (2013).
[b]Two-photon excitation starting from $3d^34s\ a^5F$. Line width 0.01 nm.
[c] All measurements were made in the second spectral order.
[d]Semi-empirical superposition-of-configurations calculation by Kurucz (1995)
[e]Semi-empirical superposition-of-configurations calculation by Kurucz (2013)
[f]Corrected for scattered laser light

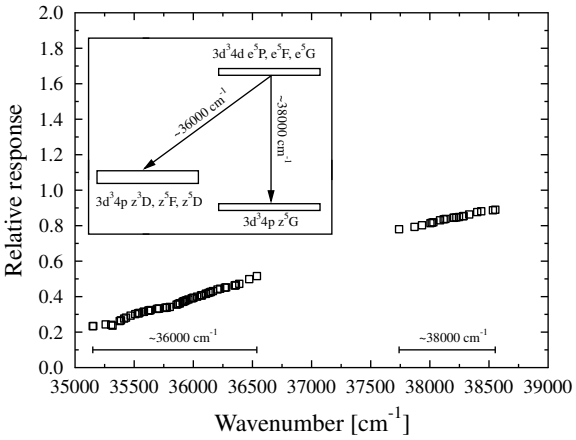

Fig. 1. Relative response of the Fourier transform spectrometer and detector. The insert shows the origin of the gap in energy between the two line groups due to the lower energy of 4p z^5G.

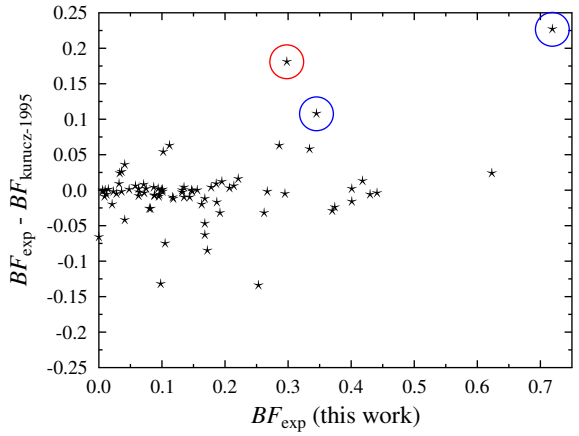

Fig. 2. All measured branching fractions for the 4p-4d transitions in V II compared with Kurucz (1995). The circled data are not calculated, but experimental values from Martin et al. (1988). See discussion in text.

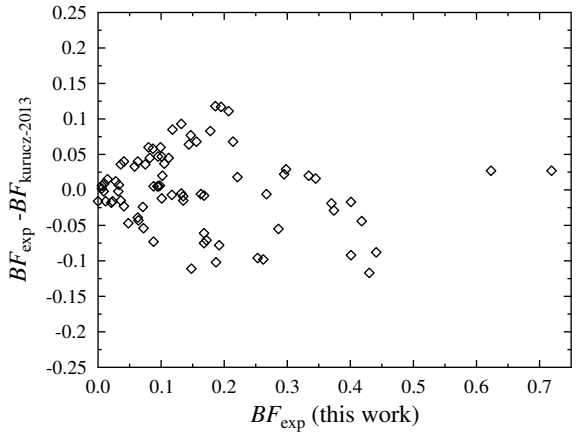

Fig. 3. All measured branching fractions for the 4p-4d transitions in V II compared with Kurucz (2013).

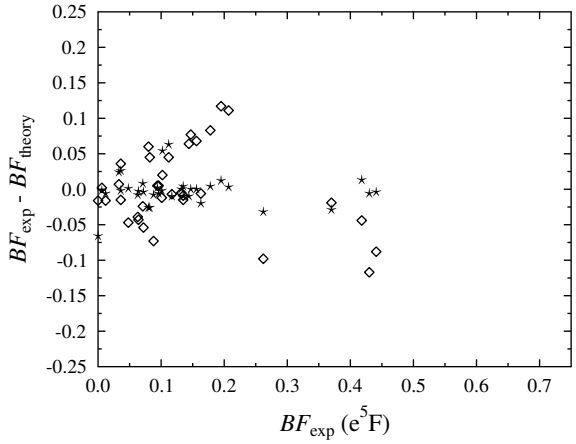

Fig. 4. The experimental branching fractions from $3d^3(^4F)4d\ ^5F$ compared with Kurucz (1995) (⋆) and Kurucz (2013) (⋄).

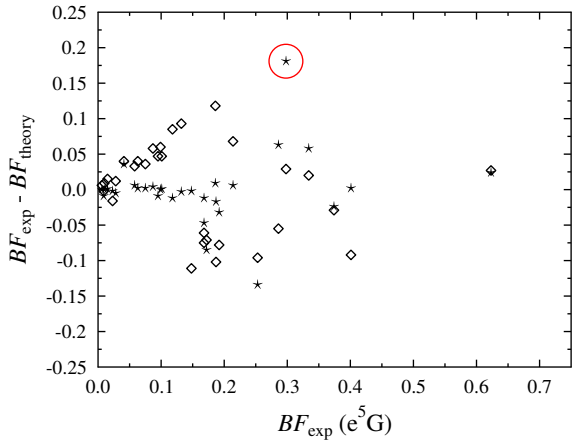

Fig. 5. The experimental branching fractions from $3d^3(^4F)4d\ e^5G$ compared with Kurucz (1995) (⋆) and Kurucz (2013) (⋄). The circled data is not calculated, but experimental values from Martin et al. (1988). See discussion in text.

Table 2. Branching fractions and oscillator strengths for $3d^3(^4F)4p–3d^3(^4F)4d$ transitions in V II

Upper level[a]	Lower level[a]	λ^a_{air} [Å]	σ^a [cm^{-1}]	BF_{exp}	Unc$_{BF}$ [%]	BF^b_{theory}	BF^c_{theory}	log(gf)$_{exp}$	Unc$_{gf}$ [%]
$3d^3(^4F)4d\ e^5P_1$	z^5D_0	2830.6580	35317.085	0.218	8.9	0.205	0.203	-0.388	12
	z^5D_1	2835.3139	35259.093	0.409	6.3	0.417	0.418	-0.128	10
	z^5D_2	2844.1564	35149.478	0.263	7.1	0.269	0.273	-0.302	11
Residual				0.110					
$3d^3(^4F)4d\ e^5P_2$	z^5F_2	2776.8557	36001.328	0.032	13.5	0.023	0.034	-1.028	16
	z^3D_2	2805.5024	35633.741	0.041	13.6	0.083	0.064	-0.908	16
	z^3D_3	2818.4608	35469.916	0.168	4.5	0.231	0.176	-0.289	9
	z^5D_1	2822.8001	35415.393	0.088	6.6	0.095	0.083	-0.571	11
	z^5D_2	2831.5654	35305.767	0.295	3.6	0.300	0.273	-0.041	9
	z^5D_3	2843.7697	35154.257	0.345	3.3	0.237	0.329	0.030	9
Residual				0.032					
$3d^3(^4F)4d\ e^5P_3$	z^3D_3	2799.9833	35703.975	0.098	6.4	0.230	0.092	-0.366	11
	z^5D_2	2812.9153	35539.839	0.021	16.6	0.041	0.039	-1.036	19
	z^5D_3	2824.9586	35388.334	0.105	6.6	0.180	0.068	-0.326	11
	z^5D_4	2825.7945	35377.866	0.719	3.1	0.492	0.692	0.508	9
Residual				0.058					
$3d^3(^4F)4d\ e^5F_1$	z^5G_2	2613.8377	38246.503	0.094	5.2	0.092	0.089	-0.818	10
	z^3D_1	2750.2255	36349.908	0.370	3.5	0.399	0.389	-0.179	9
	z^5F_2	2764.2295	36165.763	0.163	5.0	0.183	0.169	-0.530	10
	z^5F_1	2785.8843	35884.659	0.112	7.4	0.049	0.067	-0.688	11
	z^5D_0	2805.1817	35637.814	0.117	7.4	0.127	0.124	-0.661	11
	z^5D_1	2809.7551	35579.810	0.096	8.8	0.102	0.091	-0.746	12
Residual				0.048					
$3d^3(^4F)4d\ e^5F_2$	z^5G_2	2601.0539	38434.469	0.207	5.3	0.204	0.096	-0.265	10
	z^5G_3	2611.4491	38281.485	0.135	5.5	0.131	0.144	-0.447	10
	z^3D_1	2736.0767	36537.870	0.080	6.3	0.106	0.020	-0.632	10
	z^5F_2	2749.9364	36353.729	0.262	5.2	0.294	0.360	-0.114	10
	z^5F_3	2768.6482	36108.046	0.072	7.2	0.076	0.126	-0.671	11
	z^5F_1	2771.373	39072.550	bl*		0.066	0.016		
	z^3D_2	2778.0285	35986.130	0.102	6.3	0.048	0.082	-0.513	10
	z^5D_1	2794.9883	35767.780	0.048	10.7	0.047	0.095	-0.834	14
Residual				0.095					
$3d^3(^4F)4d\ e^5F_3$	z^5G_3	2603.3537	38400.518	0.146	3.1	0.154	0.080	-0.271	9
	z^5G_4	2617.0400	38199.707	0.136	3.2	0.145	0.150	-0.296	9
	z^5F_2	2740.9613	36472.761	0.083	3.8	0.108	0.037	-0.471	9
	z^5F_3	2759.5520	36227.061	0.422	1.8	0.405	0.462	0.241	8
	z^3D_2	2768.8722	36105.126	0.037	7.2	0.010	0.000	-0.820	11
	z^5F_4	2777.2875	35995.731	0.064	4.6	0.071	0.102	-0.574	9
	z^3D_3	2781.4915	35941.328	0.033	7.8	0.009	0.026	-0.859	11
	z^5D_2	2794.2532	35777.189	0.065	5.3	0.067	0.107	-0.561	10
	z^5D_3	2806.1359	35625.697	0.012	22.4	0.018	0.028	-1.302	24
Residual				0.002					
$3d^3(^4F)4d\ e^5F_4$	z^5G_3	2594.3680	38533.512	0.006	14.9	0.008	0.004	-1.558	16
	z^5G_4	2607.9594	38332.706	0.156	3.3	0.156	0.088	-0.126	7
	z^5G_5	2624.8423	38086.166	0.132	3.3	0.132	0.137	-0.195	7
	z^5F_3	2749.4562	36360.077	0.147	3.4	0.147	0.070	-0.107	7
	z^5F_4	2767.0633	36128.728	0.441	1.8	0.445	0.529	0.375	6
	z^5F_5	2782.6108	35926.872	0.036	6.1	0.038	0.051	-0.706	8
	z^5D_3	2795.7014	35758.657	0.071	4.6	0.063	0.095	-0.411	7
Residual				0.012					

Table 2. continued.

Upper level[a]	Lower level[a]	λ^{a}_{air} [Å]	σ^{a} [cm^{-1}]	BF_{exp}	Unc$_{BF}$ [%]	BF^{b}_{theory}	BF^{c}_{theory}	log(gf)$_{exp}$	Unc$_{gf}$ [%]
3d^3(^{4}F)4d e^{5}F$_5$	z^{5}G$_5$	2615.3665	38224.149	0.178	3.2	0.174	0.095	0.030	7
	z^{5}G$_6$	2635.3914	37933.721	0.101	3.4	0.103	0.113	-0.208	7
	z^{5}F$_4$	2756.5346	36266.715	0.195	3.2	0.183	0.078	0.116	7
	z^{5}F$_5$	2771.9633	36064.866	0.430	2.0	0.436	0.547	0.465	6
	z^{5}F$_4$	2785.7648	35886.198	0.088	3.9	0.096	0.161	-0.218	7
Residual				0.007					
3d^3(^{4}F)4d e^{5}G$_2$	z^{5}G$_2$	2611.1949	38285.211	0.148	2.9	0.150	0.259	-0.393	12
	z^{5}G$_3$	2621.6713	38132.230	0.015	11.2	0.014	0.000	-1.392	16
	z^{3}D$_1$	2747.2996	36388.618	0.168	3.0	0.215	0.229	-0.293	12
	z^{5}F$_2$	2761.2739	36204.472	0.118	3.6	0.130	0.033	-0.441	12
	z^{5}F$_3$	2780.1406	35958.792	0.095	4.2	0.104	0.048	-0.532	12
	z^{5}F$_1$	2782.8822	35923.368	0.286	2.4	0.223	0.341	-0.051	11
	z^{5}D$_1$	2806.7007	35618.528	0.101	4.6	0.100	0.054	-0.497	12
	z^{5}D$_2$	2815.3665	35508.899	0.058	8.4	0.052	0.025	-0.737	14
Residual				0.011					
3d^3(^{4}F)4d e^{5}G$_3$	z^{5}G$_3$	2616.6275	38205.729	0.168	2.8	0.180	0.243	-0.215	9
	z^{5}G$_4$	2630.4616	38004.809	0.041	4.2	0.005	0.001	-0.824	9
	z^{5}F$_2$	2755.6791	36277.973	0.172	2.9	0.257	0.243	-0.161	9
	z^{5}F$_3$	2774.4693	36032.291	0.099	3.6	0.099	0.039	-0.392	9
	z^{3}D$_2$	2783.8890	35910.378	0.334	2.1	0.276	0.314	0.138	8
	z^{5}F$_4$	2792.3992	35800.942	0.063	5.0	0.061	0.023	-0.588	10
	z^{5}D$_2$	2809.5498	35582.410	0.087	4.2	0.083	0.029	-0.439	9
	z^{5}D$_3$	2821.5653	35430.891	0.023	14.5	0.025	0.039	-1.022	17
Residual				0.014					
3d^3(^{4}F)4d e^{5}G$_4$	z^{5}G$_4$	2622.7132	38117.082	0.192	2.8	0.224	0.270	-0.003	9
	z^{5}G$_5$	2639.7873	37870.556	0.006	16.5	0.006	0.000	-1.471	19
	z^{5}F$_3$	2765.8594	36144.452	0.253	2.6	0.387	0.349	0.162	9
	z^{5}F$_4$	2783.6777	35913.104	0.132	3.2	0.135	0.039	-0.116	9
	z^{3}D$_3$	2787.9014	35858.697	0.298	2.4	0.117	0.269	0.239	9
	z^{5}F$_5$	2799.4125	35711.255	0.028	9.5	0.033	0.016	-0.778	13
	z^{5}D$_3$	2812.6609	35543.053	0.075	4.3	0.073	0.039	-0.354	10
	z^{5}D$_4$	2813.4894	35532.588	0.009	24.1	0.018	0.011	-1.290	26
Residual				0.007					
3d^3(^{4}F)4d e^{5}G$_5$	z^{5}D$_5$	2628.7073	38030.171	0.189	4.3	0.204	0.289	0.034	9
	z^{5}G$_6$	2648.9375	37739.747	0.010	8.6	0.010	0.001	-1.233	12
	z^{5}F$_4$	2771.3590	36072.729	0.405	4.8	0.399	0.493	0.411	9
	z^{5}F$_5$	2786.9538	35870.889	0.187	4.4	0.177	0.068	0.082	9
	z^{5}D$_4$	2800.9054	35692.222	0.216	4.3	0.208	0.146	0.148	9
Residual				0.003					
3d^3(^{4}F)4d e^{5}G$_6$	z^{5}G$_6$	2629.6758	38016.166	0.374	4.0	0.398	0.403	0.406	7
	z^{5}F$_5$	2765.6408	36147.309	0.623	2.4	0.599	0.596	0.671	6
Residual				0.003					

[a]Thorne et al. (2013).
[b]Kurucz (1995).
[c]Kurucz (2013).
*Blended with z^{5}F$_4$ - e^{5}G$_5$ (see text).